Quantifying deformation and energy dissipation of polymeric surfaces under localized impact

Georgios Constantinides [a,1], Catherine A. Tweedie [a], Doria M. Holbrook [b],
Patrick Barragan [b], James F. Smith [c], Krystyn J. Van Vliet1 [a,*]

[a] *Department of Materials Science and Engineering, Massachusetts Institute of Technology, Cambridge, MA 02139, USA*
[b] *Department of Mechanical Engineering, Massachusetts Institute of Technology, Cambridge, MA 02139, USA*
[c] *Micro Materials, Ltd., Wrexham, UK*

Abstract

The mechanical response of polymeric surfaces to concentrated impact loads is relevant to a range of applications, but cannot be inferred from quasistatic or oscillatory contact loading. Here we propose and demonstrate a set of quantitative metrics that characterizes the ability of polymers to resist impact deformation and dissipate impact energy, as well as the strain rate sensitivity of these materials to contact loading. A model which incorporates nonlinear material behavior is presented and can predict the experimentally observed deformation behavior with high accuracy. The micrometer-scale impact response of several polymers has been investigated in the velocity range of 0.7–1.5 mm/s. Two semi-crystalline polymers – polyethylene (PE) and polypropylene (PP) – characterized above the corresponding glass transition temperature T_g, and four fully amorphous polymers characterized well below T_g – polystyrene (PS), polycarbonate (PC), and low and high molecular weight poly(methyl methacrylate) or PMMA termed commercially as Lucite® (LU) and Plexiglas® (PL) – have been considered. In an inverse application, the model and experimental method provide a tool for extracting the relevant material quantities, including energy dissipation metrics such as the coefficient of restitution e. This approach can be used to determine quantitatively the impact energy absorption of polymer surfaces at elevated temperatures through T_g, as demonstrated for PS and PC over the range of 20–180 °C.
© 2008 Elsevier B.V. All rights reserved.

Keywords: Polymers; Impact; Nanoindentation

1. Introduction

The advent of depth-sensing indentation (DSI) enabled fundamental studies in the nanomechanical response of metals, ceramics, polymers, and composites, e.g., Refs. [1–7]. Current technology allows for contact-based deformation of nanoscale load and displacement resolution [8,9] and has been leveraged for both general mechanical characterization of small material volumes (e.g., thin films adhered to substrates [10–12] and free-standing nanowires [13,14]) and unprecedented access to the physics of deformation processes such as dislocation nucleation in crystals [15–20]. While DSI was originally developed for stiff

metals and ceramics, it was quickly appreciated that nanoscale deformation resolution can be of significant use in so-called "soft matter" studies, in particular for biological and polymeric surfaces. Application of such capabilities toward polymeric and biological materials, however, has largely adopted a linear elastic basis (e.g., estimation of the Young's elastic modulus E from the contact stiffness $S = dP/dh$ upon unloading according to the linear elastic analysis of Sneddon [21]) that neglects time- and rate-dependence and nonlinear material physics typical of synthetic and natural polymers. Such load and time dependence of polymers under contact has been noted [22–28] and several approaches have been considered to include assumptions of linear viscoelasticity (and, typically, phenomenological idealizations of viscoelastoplastic elements) [29–36]. A noted example is nano-DMA in which one estimates storage and loss moduli E_1 and E_2 or loss tangent tan $(\delta) = E_2/E_1$ via cyclic contact loading of a nano-to microscale material volume at a mean zero stress [37,38] or a superposed contact stress [39]. These well-

---

appreciated metrics do not necessarily characterize the material resistance to impact, which is critical for development of barrier coatings and other protective devices. In fact, energy absorption in impact processes cannot be directly ascertained though DMA-type testing. To date, these responses have been approximated by macroscale quantities such as dynamic hardness in metals [40] and the coefficient of restitution in polymers [31,33,41].

In this paper we employ a recently developed experimental approach [42] that monitors the deformation response of materials subjected to the impingement of localized loads over a range of velocities. This approach recognizes the inherent time-dependence and potential nonlinearity of deformation by enjoining the general physics of impact or energy decay with contact forces and displacements down to the nanoscale. The objective then is to consider new means by which salient mechanical characteristics and physics of small and/or constrained viscoelastic material volumes can be determined, either under application-appropriate impact energy rates or from extrapolation thereof.

2. Materials and methods

2.1. Materials

A total of six bulk polymers were subjected to localized mechanical impulse or impact loading. Two semi-crystalline polymers, polyethylene (PE) and polypropylene (PP) were characterized above the corresponding glass transition temperature T_g, and four fully amorphous polymers were characterized well below T_g: polystyrene (PS), polycarbonate (PC), and low and high molecular weight poly(methyl methacrylate) or PMMA which are termed commercially as Lucite® (LU) and Plexiglas® (PL), respectively. These polymers were obtained from DuPont
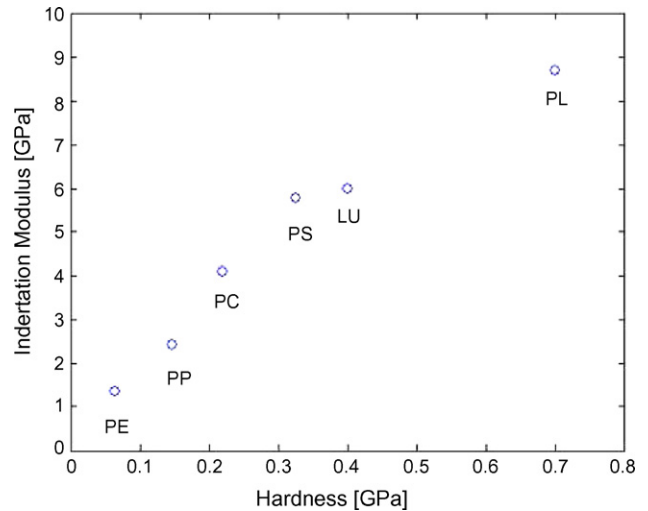

Fig. 1. Indentation moduli and hardnesses for the six polymers tested.

(Wilmington, DE) as injection moldings into smooth metal crucibles, such that the as-cooled surface finish displayed nanoscale surface roughness characterized by scanning probe microscopy in the present study. Table 1 and Fig. 1 summarize the physical (monomer structure, T_g and M_w) and mechanical properties (quasistatic indentation modulus and effective hardness) [28], respectively, of each of these bulk polymers.

2.2. Impact measurements

The operating principles of the experimental apparatus used herein are outlined in Fig. 2a. The heart of this commercially available instrumented indenter (NanoTest, Micro Materials Ltd.) is a vertical pendulum-based device in which load is
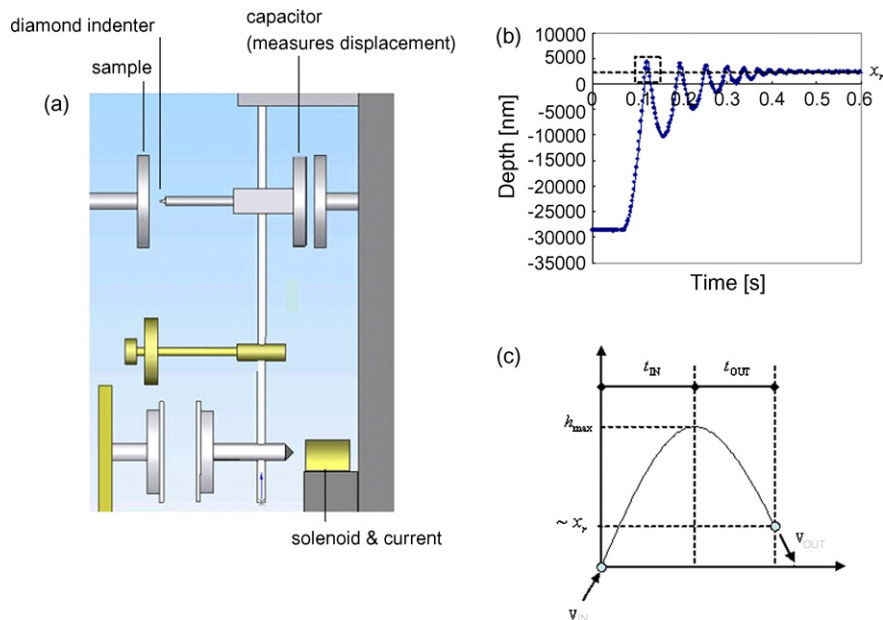

Fig. 2. (a) Experimental apparatus used to measure the impulse response and corresponding impulse energy decay. (b) Impulse response for polycarbonate (PC) at the highest impact velocity (1.5 mm/s) corresponding to an impulse energy of ∼ 250 nJ. (c) A magnified version of the first upswing into the material showing output data and characteristic variables.

Table 1
Structural/physical properties of bulk polymers used in this work

Polymer name	Structural formula	T_g (°C)	M_w (g/mol)
Polyethylene PE	+CH$_2$–CH$_2$+	−30	85,195
Polypropylene PP	+CH$_2$–CH+$_n$; CH$_3$	4.6	343,326
Polystyrene PS	+CH$_2$–CH+$_n$; C$_6$H$_5$	103	248,670
Poly(methyl methacrylate)s	+CH$_2$–C+$_n$; CH$_3$; C=O ; O ; CH$_3$		
Lucite LU[a]		114	10,42,916
Plexigilas PL[b]		117	2588.744
Polycarbonate PC	+O–C(=O)–O–C$_6$H$_4$–C(CH$_3$)$_2$–C$_6$H$_4$+$_n$	145	18.000

([a]Rohm and Haas; [b]Ineos Acrylics).

applied and measured through actuation of the pendulum around a frictionless pivot via an electromagnetic voice coil. The displacement of the indenter during load application is measured via a capacitive transducer mounted on the pendulum. Load and displacement voltage signals are independently calibrated and thermally stable. To minimize thermal drift and acoustic vibration, the entire instrument is placed within an acoustic isolation enclosure at controlled temperature (26 °C) and relative humidity (50%). In conventional indentation tests the contact loading is achieved via feedback-controlled modulation of the coil current (and thus force P), and the continuous monitoring of the load–depth (P–x) response. The extension to impact testing is outlined in Ref. [42] and is achieved via an additional component to the load train. In a typical impact test, the indenter position x is acquired continuously as a function of time t after imparting potential energy to the pendulum (using a predefined loading ramp) such that the pendulum swings and bounces on the surface of the material of interest. The energy is imparted to the pendulum using a solenoid at the pendulum end that is energized to attract the pendulum away from the surface. While the pendulum is held firmly in place by the magnet, a small force is applied through the electromagnetic voice coil. The motion indicated in Fig. 2b is achieved using a step-down change in the magnetic force that allows the pendulum to swing toward the material of interest, while the coil current that generated this motion is maintained constant.

For each material and impact velocity considered, at least five trials under identical conditions were conducted and analyzed. Pendulum displacement as a function of time $x(t)$ was recorded (see Fig. 2b), where the surface position $x = 0$ was known through calibration of the sample plane immediately prior to each impact. For the purposes of data analysis, $t = 0$ was arbitrarily assigned as the time corresponding to $x = 0$, i.e., at the start of the first impact contact. For each experiment, the following data were monitored: impact and rebound velocities v_{in} and v_{out} corresponding to the initial impact, maximum depth x_{max}, residual depth x_r, loading and unloading times t_{in} and t_{out} (see details in Fig. 2c). The residual depth was measured at the end of the impact process, being in practice the position of the indenter remaining at the indentation.

These extracted quantities are linked to material constants using a model developed below. The repeatability in $x(t)$ among experiments for a given pendulum velocity and material sample was very high. For example, the measured maximum depth x_{max} for a given velocity and material was within 5–10% for the five repetitions.

2.3. Impact analysis

Fig. 2b shows the pendulum impact trajectory during a test on polycarbonate after a step-decrease in the solenoid current that transfers an impact force to the pendulum F_{imp}, which remains constant during the test. This motion can be described

mathematically using a model developed in Ref [42]:

$$F_{imp} = m\ddot{x} + \varrho\dot{x} + kx + \mathcal{F}(x) \tag{1}$$

$$\mathcal{F}(x) = \begin{cases} 0 & \text{if} \quad x < 0 \quad \text{and} \quad \dot{x} > 0 \\ C_{in}x^2 & \text{if} \quad x > 0 \quad \text{and} \quad \dot{x} > 0 \\ C_{out}x_{max}x + (C_{in} - C_{out})x_{max}^2 & \text{if} \quad x > x_r \quad \text{and} \quad \dot{x} < 0 \\ 0 & \text{if} \quad x < x_r \quad \text{and} \quad \dot{x} < 0 \end{cases} \tag{2}$$

where F_{imp} is the impact force required to impart the initial energy into the material, C_{in} is the resistance coefficient of the material to impact loading, and C_{out} is the recovery coefficient of the material upon unloading. The resistive force $\mathcal{F}(x)$ was used in Eq. (1) to model the impact of the indenter on the surface at $x = 0$, where $\dot{x} > 0$ represents the positive velocity into the surface and x_{max} the maximum depth of indentation. The subscripts *in* and *out* denote the material quantities related to the loading and unloading portion of the indentation response. In Eq. (1), we assumed that the resistance of the material during indentation follows the quasi-static quadratic form $\sim C_{in}x^2$ [43]. For high velocities or time-dependent material behavior this assumption breaks down and the strain rate sensitivity of the material and/or the kinetic energy of the targeted specimen should be considered in the analysis. Most polymers show significant viscous behavior even in low velocity deformation, indicating strong likelihood of a non linear resistance response. Under these conditions the resistance coefficient C_{in} is not constant but becomes a function of the strain rate. To model this material response we use a function $C_{in}(\dot{x})$ of the form:

$$\mathcal{F}(x) = C_{in}(\dot{x})x^2 \tag{3}$$

$$C_{in} = C_{in}^o \left(1 + \left(\frac{1}{r}\frac{\dot{x}}{x} \right)^b \right) \tag{4}$$

where $\dot{x}/x$ is the indentation strain rate [5], C_{in}^o is the quasistatic indentation coefficient, and r and b are material constants that characterize the strain rate sensitivity of the indentation response. Eq. (3) was used in Ref. [44] to account for the dynamic hardening of metals under high velocities. It is interesting to note that for low strain rates ($\dot{x}/x \ll r$) the quadratic relationship persists. For strain rates comparable to the strain rate sensitivity of the material $\dot{x}/x \sim r$ the force scales with $\mathcal{F}(x) \sim x^{2-b}$ and an additional damping term contributes: $C_{in}^o \times (\dot{x}/r)^b \times x^{2-b}$, which dissipates energy during the impact process. Fig. 3 shows the evolution of the resistive force with depth as predicted by Eq. (3) for different indentation strain rates. For indentations with constant $\dot{x}/x$ the quadratic dependency is retained. As $\dot{x}/x$ increases the effective resistance coefficient C_{in} also increases, which thus requires greater applied force to achieve a given indentation depth. It should be noted, that during an impact test, the indentation strain rate $\dot{x}/x$ continuously changes reaching a zero value at maximum penetration depth. The constants m, ρ, and k are characteristics of the pendulum and can be obtained from a pendulum calibration process described in Ref. [42]. For the apparatus used in the present experiments, the pendulum mass m, effective internal damping coefficient ϱ,
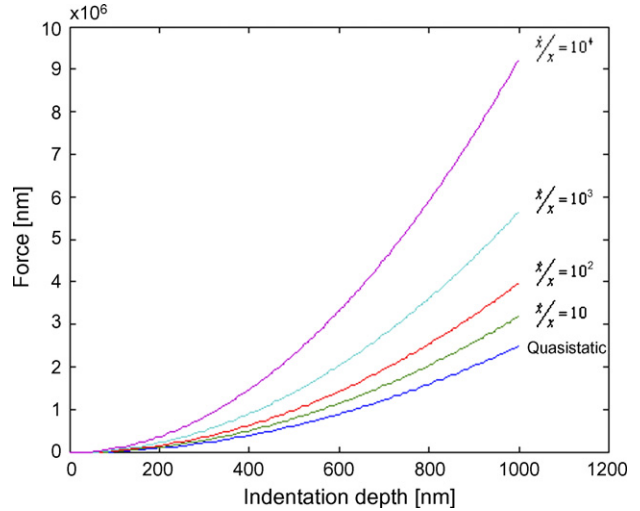

Fig. 3. Predicted resistive force as a function of penetration depth for different indentation strain rates, on a model material defined by the resistance parameters $C_{in} = 2.5\,\text{GPa}$, $r = 500\,\text{s}^{-1}$, and $b = 1/3$.

and spring constant k are:

$$m = 0.21\,\text{kg} \quad \varrho = 0.96\,\text{N s/m}, \quad k = 10\,\text{N/m} \tag{5}$$

The third condition in Eq. (2) describes a linear unloading portion of the P-x response curve as normally used for quasistatic indentation analysis. Here, we define the initial slope or tangent of the unloading curve $dP/dx = C_{out}x_{max}$ (at $x = x_{max}$) and we use the condition $P = C_{in}x_{max}^2$ at $x = x_{max}$. The definition of dP/dx is chosen for dimensional consistency, and thus C_{out} is termed the recovery coefficient. The complexity of Eq. (1) does not allow for an explicit analytical solution to be found. A numerical solution can be achieved using a developed Matlab® algorithm that utilizes the ordinary differential equation solver. The predictive capabilities of this model will be demonstrated below.

3. Results and discussion

3.1. Polymer impact experiments

Indentation impact experiments were performed on the six polymers with impact velocities in the range of 0.7–1.5 mm/s employing a diamond Berkovich indenter. The damped oscillatory response due to polymer contact is shown in Fig. 2b for the specific case of polycarbonate (PC) under an initial impact energy of 50 nJ ($v_{in} = 0.69$ mm/s). As expected intuitively, the polymer absorbs impact energy and thus strongly attenuates the successive pendulum rebound amplitudes, coming to rest after ~ 0.5 s post-impact. In addition to impact tests, quasistatic indentation tests at a maximum load of 30 mN were also performed on all six polymers; the extracted indentation moduli and hardness are listed in Table 2. The loading/unloading rate was varied to ensure that the extracted elastic moduli are representative of the instantaneous moduli of the material and unaffected by the viscous deformation. In fact, as we increased the unloading rate (from 0.056 mN/s to 1.50 mN/s) the instantaneous

Table 2
Subset of key quasistatic and impulse indentation results for amorphous polymers

	E (GPa)	H (GPa)	C_{in}^o (GPa)	E/H (−)	r (1/s)	b (−)	e (−)
PE	1.36	0.07	1.23	21	–	–	0.62
PS	5.79	0.33	5.82	17	–	–	0.64
PC	4.10	0.22	3.98	19	–	–	0.65
PP	2.41	0.15	2.47	16	500	1/3	0.66
PL	8.70	0.70	11.03	12	–	–	0.68
LU	6.00	0.40	6.76	15	10–100	1/3	0.70

unloading slope became constant and independent of the rate of load removal. The resistance coefficient C_{in}^o which is used in the numerical solution of our model, Eq. (1), was calculated through [45]:

$$C_{in}^o = E_r \left[\frac{1}{\sqrt{\kappa}} \sqrt{\frac{E_r}{H}} + \left(\frac{2(\pi-2)}{\pi} \right) \sqrt{\frac{\pi}{4}} \sqrt{\frac{H}{E_r}} \right]^{-2} \qquad (6)$$

where $\kappa = 3\sqrt{3}\tan^2\theta$ is a geometric constant ($\kappa = 24.56$ for Berkovich indenters as used here), H is the quasistatic hardness of the material defined as the maximum load over the projected area of contact, and E_r is the effective indentation modulus which is approximately equal to the plane strain modulus of the indented material $E/(1 − \nu^2)$; H and E were obtained from quasi-static indentation. Eq. (6) was obtained using finite element simulations of elastic–plastic conical indentation [46]. The C_{in}^o-values calculated for all six polymers are summarized in Table 2.

The quasistatic form of Eq. (1) was used in Ref. [42] on impact indentation of aluminum and showed excellent predictive capabilities. In what follows, the quasistatic predictions of Eq. (1) are compared with our experimental data on polymers. In cases where deviation exists, the strain rate parameters r and b are modified such that the numerical simulations match the experimentally observed response. In doing so, we assume that any deviation between simulations and experiments is due to an apparent strain rate sensitivity that is captured by the form of Eq. (3).

3.1.1. Maximum depth of penetration and residual imprint

Figs. 4 and 5 compare the maximum indentation depth for the five pendulum upswing velocities for all six polymer samples. During the loading phase of the contact impact the indenter is damped by a resistive force generated by the material in reaction to the indenter moving in at the given velocity. The maximum penetration inside the material scales with $x_{max} \sim v_{in}^{2/3}/C_{in}$. Of the polymers examined, polyethylene (PE) and polypropylene (PP) were the only samples tested above their T_g and were deformed the most upon first pendulum impact, indicating that ambient temperature relative to glass transition temperature, is a strong determinant of instantaneous impact resistance. Amorphous polycarbonate (PC), polystyrene (PS), Plexiglas®(PL), and Lucite®(LU) vary in molecular weight M_w by an order of magnitude, and yet exhibited a similar depth of indentation upon the initial impact $x(t = 0)$, suggesting that molecular weight is a weak determinant of impact resistance or energy absorption

for all home polymers impacted below T_g. In fact, PL possessed a M_w more than twice that of LU, but exhibited only a slightly smaller $x(t = 0)$ for the same impact force F_{imp}. Table 2 summarizes the metrics of energy absorption extracted from such responses for these polymers over the range of conditions considered.

Fig. 4 shows the quasistatic numerical predictions for PC, PS, PE and PL. The close agreement between experiments and simulations for all the velocities considered herein suggest these 4 polymers exhibit minimal strain rate sensitivity within the mm/s velocity range tested. In contrast, PP and LU significantly deviated from the quasistatic response (see Fig. 5). The coefficients r and b in Eq. (3) were adjusted to fit the experimental response. In doing so, we assumed that the deviation between experimental data and numerical simulations was due to the strain rate sensitivity of the material that was not accounted for in the quasistatic analysis. A sensitivity analysis of these fits showed that, for the given C_{in} and velocity range, the maximum indentation depth x_{max} versus the incident velocity v_{in} response is relatively insensitive to the exact value of b and is primarily driven by the strain rate material constant r. This is illustrated in Fig. 6. In the fitting process for PP and LU, b was therefore assumed constant at $b = 1/3$. The extracted coefficients are listed in Table 2.

While r and b characterize the strain rate sensitivity of the material to indentation response, the link between these parameters and with other commonly employed mechanical metrics
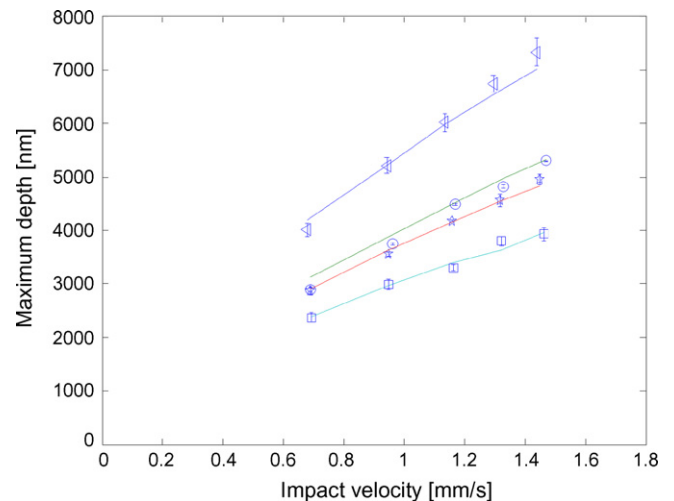

Fig. 4. Maximum depth of penetration for five different impact velocities. Experimental data: PE (c), PC ($\circ$), PS ($\star$), PL (#), and quasistatic ($r \to \infty$) numerical simulations (—).
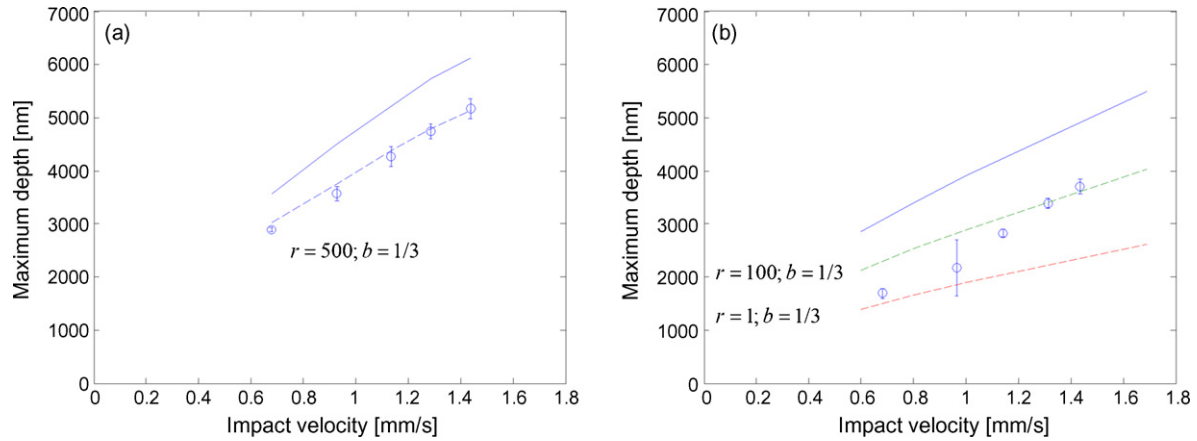
Fig. 5. Quasistatic (–) and strain rate sensitive (−−) predictions of the experimental data on (a) polypropylene (PP) and (b) Lucite (LU).

remains to be established. Andrews et al. [44] performed finite element simulations for a range of elasto–plastic materials (classical von Mises elastoplasticity with constant strain hardening) and found that $r \simeq 40\dot{\varepsilon}_o c$ and $b \simeq c$ where c and $\dot{\varepsilon}_o$ are material constants that characterize the amplification effect of the dynamic strength σ_y, normalized by the quasi-static strength σ_y^o which is commonly accounted for through the dimensionless function:

$$\sigma_y/\sigma_y^o = \left(1 + \left(\frac{\dot{\varepsilon}}{\dot{\varepsilon}_o}\right)^c\right) \tag{7}$$

Macroscopic experimental data on polymers shows similar scaling behavior of flow stress with the strain rate as the one expressed in Eq. (7)[47]. Most polymers, however, exhibit significant viscoelastoplastic behavior and the link between parameters r and b and other commonly used material constants (i.e., viscosity coefficients, time constants etc.) might therefore include not only the strength coefficients $\dot{\varepsilon}_o$ and c but also coefficients characterizing the viscous response. Although beyond the focus of the current study, finite element simulations with appropriate strain-sensitive viscoelastoplastic models can facilitate the bridge between r and b and relevant material properties, and can also quantify the relative contributions of viscous and plastic deformation under impact. Simple scaling arguements, however, suggest that viscous deformation does not significantly contribute to the overall impact response. Quasistatic creep experiments on the same polymers tested herein [28] indicate an initial creep rate of 10^2–10^4 nm/s. The indentation duration of our experiments (during first impact) is on the order of 10^{-2}–10^{-3} s, giving a maximum creep displacement of 1–100 nm. This contribution represents $< 5\%$ of the maximum displacement observed upon impact $x_{\max}$ (see Figs. 4 and 5).

Fig. 7 shows the residual depth left on the surface of the polymers after impact x_r versus the maximum penetration depth $x_{\max}$ for the six polymers considered in this study. The experimental data falls in almost perfect straight lines for all of these polymers. This is consistent with the simplified one-dimensional model presented in Ref. [44] and experiments on metals presented in Ref. [42]. Furthermore, this linear scaling appears to be insensitive to the strain rate sensitivity of the material. Quasistatic elastoplastic results presented by Giannakopoulos and Suresh [48], which were obtained using finite element simula-
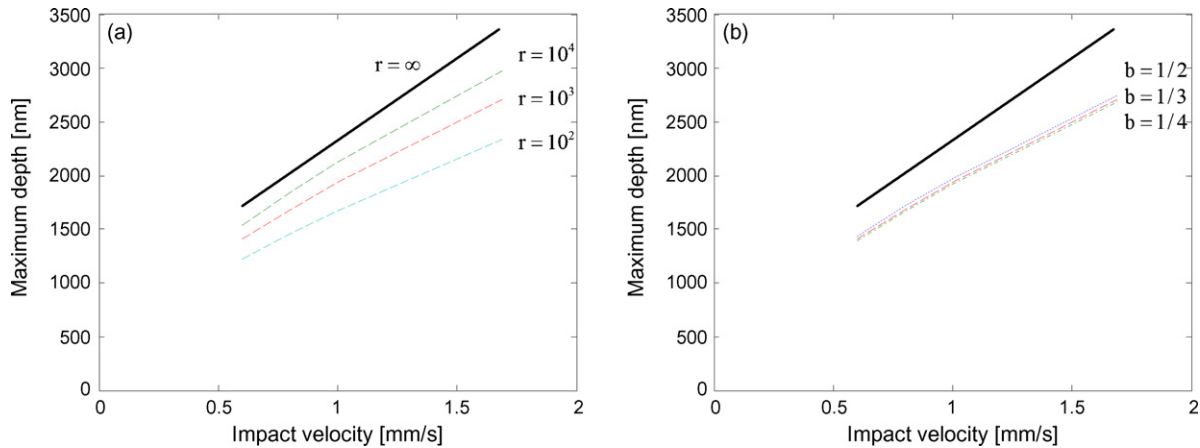

Fig. 6. Sensitivity analysis of the calculated maximum depth versus incident velocity response ($x_{\max}$ versus v_{in}) for different values of (a) r, $r = 10^2, 10^3, 10^4, \infty$ (s^{-1}) and (b) b, $b = 1/2, 1/3, 1/4$ (-). The resistance coefficient used for the numerical calculations was $C_{in} = 5$ GPa. Quasistatic (–) and strain rate sensitive results (−−).
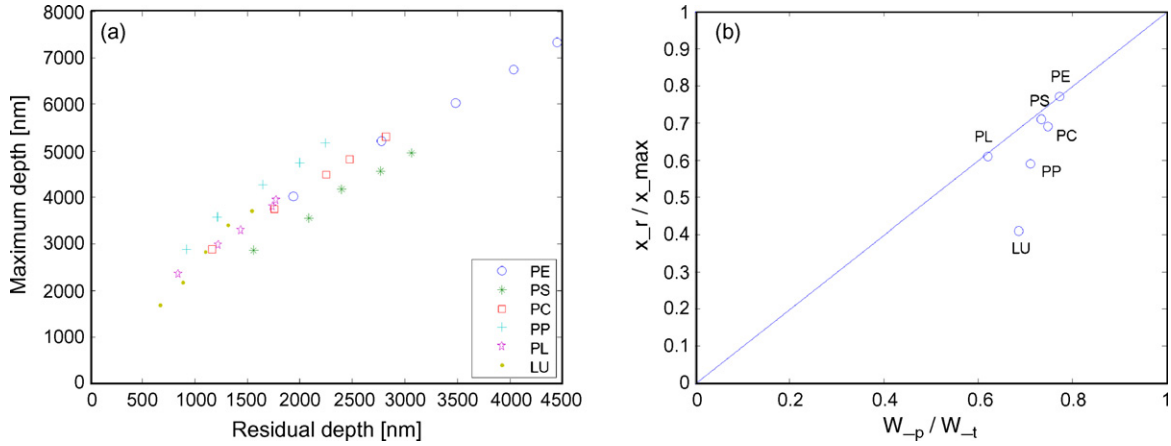
Fig. 7. (a) Maximum depth versus residual indentation depth for the six different polymers considered in this study. (b) Normalized residual depth x_r/x_{max} versus W_p/W_t for the six polymers.

tions, suggest that:

$$x_r/x_{max} = 1 - d^* \frac{H}{E_r} = \frac{W_p}{W_t} \tag{8}$$

where d^* is a constant which depends on the indenter geometry ($d^* = 5$ for Vickers and $d^* = 4.7$ for Berkovich), H and E_r are the quasistatic hardness and effective indentation modulus defined in Eq. (6), W_p and W_t are the plastic and total work done during indentation, with $W_t = \int_0^{x_{max}} P(x)dx$. The validity of Eq. (8) is examined in Fig. 7b. The experimentally obtained normalized residual depth x_r/x_{max} is compared to the normalized energy dissipation W_p/W_t. The latter quantity is calculated through $1 - d^* \times (H/E_r)$, using the quasistatic indentation results presented in Table 2. It is interesting to note that PP and LU, the two materials that demonstrated strain rate sensitive impact resistance, deviate from the line of equality, while the other four glassy polymers (PS, PC, PE, PL) show very good agreement with this energy dissipation equivalence. This suggests that other sources of energy dissipation than von Mises-type plasticity contribute to the response of PP and LU.

3.1.2. Coefficient of restitution e

A useful quantity to express the energy loss during impact is the coefficient of restitution e, defined as:

$$e = \left| \frac{v_{out}}{v_{in}} \right| \tag{9}$$

where v_{in} is the incident speed of the indenter and v_{out} the rebound speed. The parameter e has been found useful in measuring the dissipation of energy during the collision of many objects, materials and surfaces [49]. Generally, the coefficient of restitution is a measure of the elasticity of the collision ($e = 1$). In fact, e can be recast in the form:

$$K = \frac{((1/2)mv_{in}^2 - (1/2)mv_{out}^2)}{(1/2)mv_{in}^2} = 1 - e^2 \tag{10}$$

which is equivalent to the relative loss of kinetic energy dissipated during an impact with $(1/2)mv_{in}^2$, $(1/2)mv_{out}^2$ being

(approximately)[2] the total energy of the system before and after the collision. For an elastic collision where zero energy is lost, e will therefore be equal to unity and K will be zero. It is therefore apparent that the coefficient of restitution is a measure of the material energy dissipation per impact.

The coefficient of restitution of the pendulum-polymer system e was calculated by differentiating the measured displacement-time response and was observed to be independent of impact energy (i.e., of v_{in}) over the range of F_{imp} considered herein. In fact, for the polymers considered, e ranged from 0.64 (PS) to 0.70 (LU) for the amorphous polymers and 0.62 (PE) and 0.66 (PP) for the semi-crystalline polymers (see Fig. 8). Although e is not strictly equivalent to the coefficient of restitution of the material itself, but rather of the pendulum as damped by the sample surface, it is clear that the dissipative capacity of the material dominates and e is robust and correlative with the monomer type and the T_g and M_w of a given polymer. Specifically, LU and PL have the highest M_w and also the highest values of e. Although the low standard deviation of e for a given polymer implies statistically significant differences in e for the six polymers considered, the magnitude of e did not depend strongly on any single polymer attribute. In general, higher M_w correlated with an increase in e, but no clear effect of crystallinity, monomer structure, or T_g was apparent.

---

[2] The energy input to the system by imparting it to its initial position $x(0)$ and giving it an initial velocity $\dot{x}(0)$ is the sum of the kinetic and potential energy:

$$T = \frac{1}{2}k[x(0)]^2 + \frac{1}{2}m[\dot{x}(0)]^2$$

Within domain A the energy can be calculated by considering the experimentally obtained $x(t)$ and $\dot{x}(t)$ in the above equation. When the pendulum first hits the material surface the potential energy of the system is zero and the total energy is equivalent of the kinetic energy $E_{total} = (1/2)mv_{in}^2$. During the rebound phase the material loses contact earlier approximately at $h = h_r$ and as a consequence the total energy is equivalent to $E_{total} = (1/2)mv_{out}^2 + (1/2)kh_r^2 \simeq (1/2)mv_{out}^2$ for the velocities considered herein.
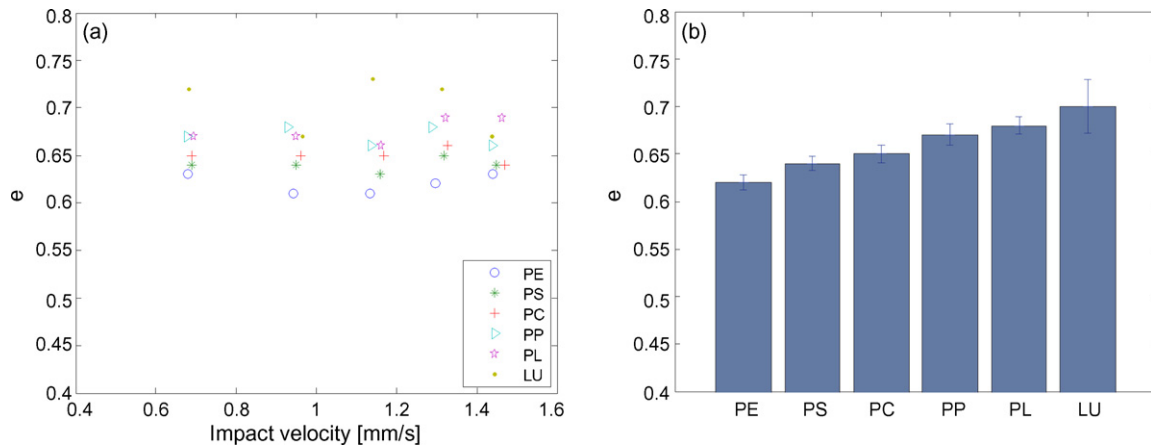
Fig. 8. (a) The coefficient of restitution as a function of impact velocity. (b) Mean values for the six polymers tested: polyethylene (PE) and polypropylene (PP) and four amorphous polymers (polycarbonate (PC), Plexiglas® (PL), Lucite® (LU) and polystyrene (PS)).

3.2. Impact resistance at elevated temperature

As a case study of the described testing methodology, we measured the evolution of impact resistance as extracted from impact analysis of $x(t)$ at elevated temperatures. Two amorphous polymers (polystyrene (PS) and polycarbonate (PC)) were subjected to the impact energy characterization technique presented above at temperatures ranging from room temperature up to 125% of their glass transition temperature T_g. Similar to room temperature testing, for each material and impact velocity considered, at least five trials under identical conditions were conducted and analyzed. The experiments were highly repeatable, as illustrated in Fig. 9a, which includes five repetitions for the impact tests on PS at an impact velocity of $v_{in} = 1.5$ mm/s. For each experiment, the coefficient of restitution e and resistance coefficient C_{in} were extracted, using Eq. (9) and the numerical solution of Eq. (1), respectively. The effect of temperature on these quantities is substantiated in Figs. 10 and 11.

Fig. 9b shows the change in the $x(t)$ response as a function of temperature. It is apparent that as the temperature increases, the material tends to damp the pendulum impact more quickly and dissipates the imparted energy in fewer cycles. This trend is consistent with the concept that the capacity of the polymer surface to dissipate energy increases as glass transition temperature is approached. This is further illustrated through the evolution of the coefficient of restitution (Fig. 10). The coefficient of restitution for PC and PS obtained at two impact velocities ($v_{in} = 0.69$ mm/s (○) and $v_{in} = 1.5$ mm/s (*)) is shown as a function of normalized temperature T/T_g. While e remains approximately constant in the region $T < T_g$, it drops dramatically for $T > T_g$. This is consistent with the increased mobility of chains at temperatures greater than the glass transition temperature. The material can therefore more easily deform and convert the imparted energy into viscous permanent dissipation and/or deformation. Furthermore and consistent with the one-dimensional impact theory, the change in e with temperature $e(T)$ is independent of impact velocity. In fact, polystyrene considered at two different velocities (corresponding to two different impact energies) exhibits an almost identical response (see Fig. 10).

Similar to e, the coefficient of impact resistance C_{in} decreases with increasing temperature, with this effect being more pronounced in the region $T > T_g$ (Fig. 11). This suggests that both strength and elasticity properties degrade in a similar fashion
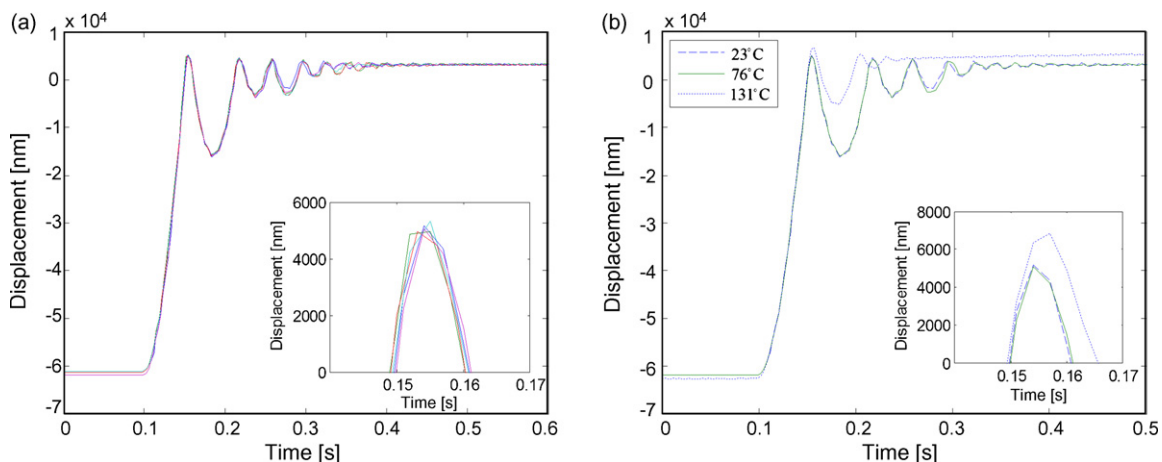

Fig. 9. (a) Repeatability of $x(t)$ impulse curves on polystyrene specimens tested at an impact velocity of $v_{in} = 1.5$ mm/s. (b) Effect of ambient temperature on $x(t)$ response. Experiments on polystyrene tested at an impact velocity of $v_{in} = 1.5$ mm/s.
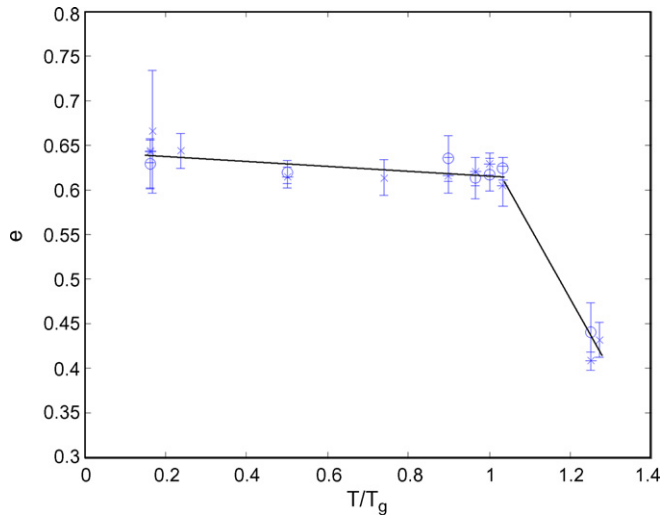
Fig. 10. Evolution of coefficient of restitution as a function of temperature. Results on polystyrene tested at $v_{in} = 1.5$ mm/s ($\times$) and polycarbonate tested at $v_{in} = 0.69$ mm/s ($\circ$) and $v_{in} = 1.5$ mm/s ($*$). Solid lines are linear fittings of the experimental data in the two different temperature regimes: $T < T_g$ and $T > T_g$.

with increasing temperature. Furthermore, $C_{in}(T/T_g)$ is quite similar for both polymers (PS and PC), provided the response is normalized by their respective glass transition temperatures. Impulse loading performed at room temperature after the materials had been exposed to temperatures $T > T_g$ demonstrated almost identical results to those obtained before heating these polymers, suggesting that the mechanisms responsible for the mechanical property degradation are fully reversible upon return to testing temperatures $T < T_g$. Certainly rigorous identification of the competing mechanisms by which energy is dissipated in these different polymers required further study, which can be enabled by this experimental approach and analysis.
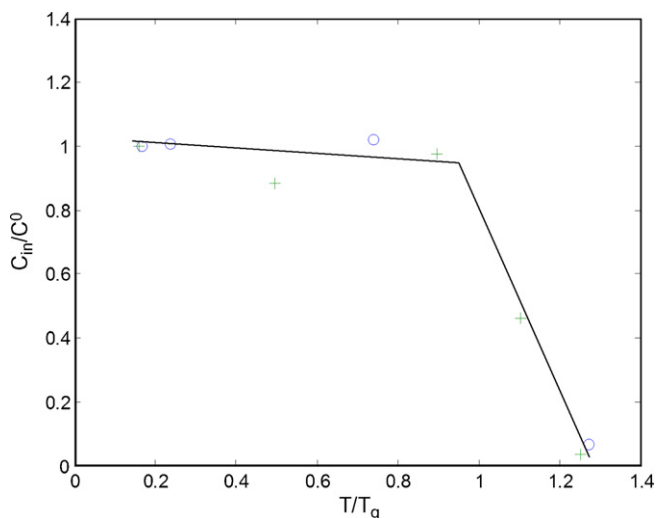

Fig. 11. Coefficients of resistance normalized with their room temperature counterparts plotted as a function of temperature normalized by their glass transition temperatures for the two specimens tested: polystyrene ($\circ$) and polycarbonate (+). Solid lines are linear fittings of the experimental data in the two different temperature regimes: $T < T_g$ and $T > T_g$.

4. Conclusions

The indentation-enabled impact approach detailed herein extracts several unique metrics of material-dependent deformation in viscoelastic–plastic materials, without assuming constitutive or phenomenological models of viscoelastic response *a priori*:

1. A numerical model describing the motion of the indenter has been provided and found to correlate well with the experimental response. It also provides the means to quantify the strain rate sensitivity of these polymers.
2. Among the six polymers tested, only polypropylene (PP) and Lucite (LU) exhibited strong strain rate sensitivity under impact for the considered range of impact energies/rates.
3. The maximum penetration depth x_{max} was found to scale linearly with the residual depth x_r for all six polymers, irrespective of material strain rate sensitivity. The ratio x_r/x_{max} is related directly to the percentage of total impact energy dissipated via an elastic deformation of the material, W_p/W_t, for all but the two polymers that exhibited strong strain rate sensitivity under impact (PP and LU).
4. A coefficient of restitution e of the pendulum was calculated and found to be independent of the impact velocity over the range considered, and is driven by the indenter geometry (which dictates strain magnitude) and characteristics of the impacted material.
5. The high temperature impact response of PS and PC was measured for values exceeding the glass transition temperature of the material. The capacity of the material to dissipate energy during impact (quantified through the resistance coefficient C_{in} and coefficient of restitution e) greatly increases for temperatures exceeding the glass transition temperature of the material $T > T_g$. Furthermore the mechanisms responsible for this change with temperature are fully reversible upon return to room temperature $T < T_g$.

These findings indicate that indentation impact characterization can provide several quantitative measures of viscoelastic–plastic energy dissipation that correlate with structural and physical characteristics of polymeric materials. Nanoscale-resolution impact testing can thus provide accurate, constitutive model-free characterization of polymer surface and thin film performance. This methodology complements current quasistatic approaches and is particularly well-suited to recapitulation of in-service conditions requiring energy dissipation or damage-tolerance of polymer surfaces.

Acknowledgements

References

[1] W.C. Oliver, G.M. Pharr, J. Mater. Res. 7 (1992) 1564–1583.

[2] T.F. Page, W.C. Oliver, C.J. Mchargue, J. Mater. Res. 7 (1992) 450–473.

[3] M. Dao, N. Chollacoop, K.J. van Vliet, T.A. Venkatesh, S. Suresh, Acta Mater. 49 (2001) 3899–3918.

[4] M.R. VanLandingham, J.S. Villarrubia, W.F. Guthrie, G.F. Meyers, Macromol. Symp. 167 (2001) 15–43.

[5] Y.T. Cheng, C.M. Cheng, Mater. Sci. Eng. R 44 (2004) 91–149.

[6] G. Constantinides, K.S.R. Chandran, F.J. Ulm, K.J. Van Vliet, Mater. Sci. Eng. A 430 (2006) 189–202.

[7] G. Constantinides, F.J. Ulm, J. Mech. Phys. Solids 55 (2007) 64–90.

[8] G.M. Pharr, W.C. Oliver, MRS Bull. 17 (1992) 28–33.

[9] G.M. Pharr, Mater. Sci. Eng. A 253 (1998) 151–159.

[10] A.K. Bhattacharya, W.D. Nix, Int J. Solids Struct. 24 (1998) 1287–1298.

[11] W.D. Nix, Mater. Sci. Eng. A 234 (1997) 37–44.

[12] R. Saha, W.D. Nix, Acta Mater. 50 (2002) 23–38.

[13] M.F. Savage, J. Tatalovich, M. Zupan, K.J. Hemker, M.J. Mills, Mater. Sci. Eng. A 319 (2001) 398–403.

[14] J.R. Greer, W.D. Nix, Apppl. Phys. A 80 (2005) 1625–1629.

[15] E.B. Tadmor, R. Miller, R. Phillips, M. Ortiz. J. Mater. Res. 14 (1999) 2233–2250.

[16] K.J. Van Vliet, J. Li, T. Zhu, S. Yip, S. Suresh, Phys. Rev. B 67 (2003) 104105.

[17] E.T. Lilleodden, J.A. Zimmerman, S.M. Foiles, W.D. Nix, J. Mech. Phys. Solids 51 (2003) 901–920.

[18] A.M. Minor, E.T. Lilleodden, E.A. Stach, J.W. Morris, J. Mater. Res. 19 (2004) 176–182.

[19] M. Fago, R.L. Hayes, E.A. Carter, M. Ortiz, Phys. Rev. B 70 (2004) 100102.

[20] A.C. Lund, A.M. Hodge, C.A. Schuh, Appl. Phys. Lett. 85 (2004) 1362–1364.

[21] I.N. Sneddon, Int. J. Eng. Sci. 3 (1965) 47–57.

[22] B.J. Briscoe, P.D. Evans, S.K. Biswas, S.K. Sinha, Tribol. Int. 29 (1996) 93–104.

[23] B.J. Briscoe, K.S. Sebastian, Proc. R. Soc. Lond. Ser. A 452 (1946) 439–457.

[24] M.R. VanLandingham, S.H. McKnight, G.R. Palmese, J.R. Elings, X. Huang, T.A. Bogetti, R.F. Eduljee, J.W. Gillespie, J. Adhes. 64 (1997) 31–59.

[25] I.M. Low, Mater. Res. Bull. 33 (1998) 1753–1758.

[26] I.M. Low, G. Paglia, C. Shi, J. Appl. Polym. Sci. 70 (1998) 2349–2352.

[27] C.A. Tweedie, K.J. Van Vliet, J. Mater. Res. 21 (2006) 3029–3036.

[28] C.A. Tweedie, K.J. Van Vliet, J. Mater. Res. 21 (2006) 1576–1589.

[29] Y-H. Pao, J. Appl. Phys. 26 (1955) 1083–1088.

[30] E.H. Lee, Q. Appl. Math. 13 (1955) 183–190.

[31] J.P.A. Tillett, Proc. R. Soc. Lond. Ser. B 67 (1955) 677–688.

[32] E.H. Lee, J.R.M. Radok, J. Appl. Mech. 27 (1960) 438–444.

[33] S.C. Hunter, J. Mech. Phys. Solids 8 (1960) 219–234.

[34] T.C.T. Ting, J. Appl. Mech. 88 (1966) 845–854.

[35] M.L. Oyen, R.F. Cook, J. Mater. Res. 18 (2003) 139–150.

[36] M.L. Oyen, J. Mater. Res. 20 (2005) 2094–2100.

[37] S.A.S. Asif, K.J. Wahl, R.J. Colton, O.L. Warren, J. Appl. Phys. 90 (2001) 1192–1200.

[38] G. Bar, R. Brandsch, M.H. Whangbo, Langmuir 14 (1998) 7343–7348.

[39] J.L. Loubet, W.C. Oliver, B.N. Lucas, J. Mater. Res. 15 (2000) 1195–1198.

[40] G. Sughash, H. Zhang, J. Mater. Res. 22 (2007) 478–485.

[41] K. Neideck, W. Franzel, P. Grau, J. Macromol. Sci. Phys. B38 (1999) 669–680.

[42] G. Constantinides, C.A. Tweedie, N. Savva, J.F. Smith, K. J. Van Vliet, Exp. Mech., in review.

[43] D. Tabor, Proc. Roy. Soc. A 192 (1948) 247–274.

[44] E.W. Andrews, A.E. Giannakopoulos, E. Plisson, S. Suresh, Int. J. Solids Struct. (2002) 281–295.

[45] A.C. Fisher-Cripps, Nanoindentation, 2nd ed., Springer-Verlag, Berlin, Germany, 2004.

[46] S.V. Hainsworth, H.W. Chandler, T.F. Page, J. Mater. Res. 11 (1996) 1987–1995.

[47] S. Sarva, A.D. Mulliken, M.C. Boyce, Int. J. Solids Struct. 44 (2007) 2381–2400.

[48] A.E. Giannakopoulos, S. Suresh, Scripta Mater. 40 (1999) 1191–1198.

[49] R. Cross, Am. J. Phys. 67 (1999) 222–227.